Multirobot control with double-integrator dynamics and control barrier functions for deformable object transport

Rafael Herguedas, Miguel Aranda, Gonzalo López-Nicolás, Carlos Sagüés and Youcef Mezouar

Abstract— In this paper, we propose a formation control system for deforming and transporting simultaneously a deformable object with a team of robots, modeled with double-integrator dynamics. The goal is to reach a target configuration, defined as a combination of shape, scale, orientation and position of the formation. We augment this controller with a set of control barrier functions (CBFs). The CBFs allow us to satisfy fundamental constraints for the success of the task: avoidance of agent-to-agent, agent-to-obstacle and object-to-obstacle collisions, and of excessive stretching. We test the performance of our proposal in different simulation scenarios.

I. INTRODUCTION

In recent times, we are witnessing a growing interest towards developing autonomous systems with the capacity of controlling the position and shape of flexible loads. Whether from domestic or industrial perspectives, numerous robotic techniques have been developed for executing tasks like grasping deformable objects, cloth folding and rope knotting among others [1], [2]. The high complexity of these manipulation tasks often requires the coordinated action of multiple agents, specially if the object is large, fragile, heavy or the task is challenging in terms of dexterity [3], [4].

Formation control, which is one of the most actively studied topics in multi-agent systems [5], naturally arises as an effective solution for driving a team of robots to a desired configuration. In this field, we can find linear control approaches, which are easier to handle and faster to compute than the nonlinear ones. This idea was exploited by Aranda *et al.* in their formation controller [6]. This controller allows to drive a 2D deformable object to a target configuration, defined as a combination of size, orientation, centroid position and relative distances between the agents grasping the object. Dimarogonas and Kyriakopoulos analyzed the connection between formation infeasibility and velocity alignment with a linear consensus algorithm [7]. Fathian *et al.* developed a linear distributed controller in which communication between the team members is not required, for agents with

R. Herguedas, G. López-Nicolás and C. Sagüés are with Instituto de Investigación en Ingeniería de Aragón, Universidad de Zaragoza, Spain. {rherguedas, gonlopez, csagues} @unizar.es

M. Aranda and Y. Mezouar are with CNRS, Clermont Auvergne INP, Institut Pascal, Université Clermont Auvergne, F-63000 Clermont-Ferrand, France. {miguel.aranda, youcef.mezouar} @sigma-clermont.fr
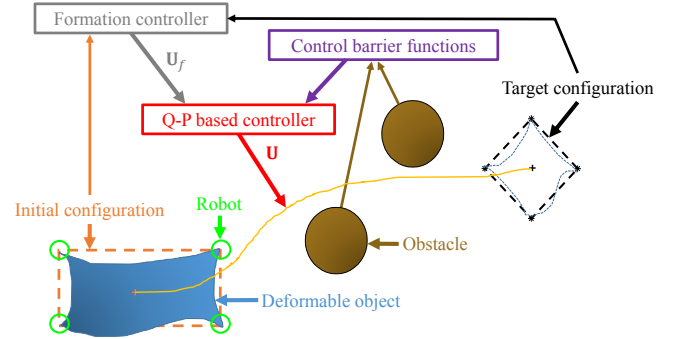
Fig. 1. The goal of our system is to steer the robotic team with the grasped object to the target configuration, defined as a combination of shape, scale, orientation and position of the formation. Our formation controller, which drives the system to the target configuration, is augmented with control barrier functions to avoid collisions and overstretching the object.

linear holonomic dynamics [8]. Affine formation controllers, whose formulation is not necessarily linear, converge to a configuration that represents an affine transformation of the desired one. Lin *et al.* proposed one of the first works about affine formation control [9]. In their proposal, the authors provided necessary and sufficient conditions for stability of the controller. A leader-follower distributed strategy by Zhao [10] is able to track a desired formation with a controller that is suitable for agents with different dynamic models. Zhao *et al.* also included motion constraints in a different proposal for rendezvous and formation control [11].

The specific tasks of shape control and transport of deformable objects are tackled in a wide variety of proposals. Felix-Rendon *et al.* proposed a multirobot centralized control scheme for controlling the position and orientation of the agents to deform an object [12]. A hybrid centralized-distributed approach by Alonso-Mora *et al.* develops a motion planning strategy of a team of robots that manipulate a deformable object [13]. In this case, collision avoidance and shape maintenance are guaranteed by a set of linear and quadratic constraints. Another hybrid approach that combines planning, control and deadlock prediction by McConachie *et al.* is able to complete complex manipulation tasks [14]. A system for simultaneous shape control and transport of deformable objects was presented in [15]. In that study, suitable trajectories were obtained according to the non-holonomic constraints of the robots and the admissible deformation states of the object, without considering collision avoidance.

Safety is one of the major concerns in robotic systems. Control barrier functions (CBFs) represent an effective and

minimally invasive technique to implement provably safe behaviors in systems with nominal, and potentially *unsafe*, control laws. These functions are currently applied in many different contexts, like collision-free multi-UAV transport of rigid payloads [16], stochastic systems [17] and safe motion control of robotic guides [18], among others.

In this paper, we build our proposal upon a recent study [19]. This study developed a formation controller for multi-agent systems with single-integrator dynamics that allows steering a team of robots, which carry a 2D deformable object, to a desired configuration. That controller is well suited for the considered scenario because it creates tightly coordinated and optimal motions. Our approach extends this previous work with a new double-integrator formulation of the formation controller. Despite the technical challenges that arise (more complex structure of the controllers, more difficult system integration...), this extension is interesting for the addition of inertial effects to the system, which are important in many practical scenarios. It also brings about the potential to control the robot-object contact forces. Moreover, being able to set the robots' accelerations is key for avoiding collisions [20]. We augment our nominal controller with CBFs, that allow us to guarantee agent-to-agent, agent-to-obstacle and object-to-obstacle collision avoidance, as well as to prevent overstretching the object. Figure 1 shows an overview of our proposal. The main contributions in the present study are a novel formation controller for agents with double-integrator dynamics, the formal proof of stability of the formation controller's shape term, and the set of CBFs for object-to-obstacle collision and overstretching avoidance.

II. PROBLEM STATEMENT

Let us consider a formation of N robots carrying a deformable object in $\mathbb{R}^2$. $\mathbf{P}_i = [P_{ix}, P_{iy}]^\intercal$, $i = 1, ..., N$ denotes the center of agent i. For every agent, we assume the object is attached to it at that center point. We stack the agents' centers in a matrix $\mathbf{P} = [\mathbf{P}_1, \mathbf{P}_2, ..., \mathbf{P}_N] \in \mathbb{R}^{2 \times N}$. The centroid of the formation is $\mathbf{g} = \frac{1}{N}\mathbf{P}\,\mathbf{1}_N$, where $\mathbf{1}_N$ is a column vector of N ones. We consider the double-integrator model to describe the robots' dynamics:

$$\begin{bmatrix} \dot{\mathbf{P}}_i \\ \ddot{\mathbf{P}}_i \end{bmatrix} = \begin{bmatrix} \mathbf{0} & \mathbf{I}_{2\times 2} \\ \mathbf{0} & \mathbf{0} \end{bmatrix} \begin{bmatrix} \mathbf{P}_i \\ \dot{\mathbf{P}}_i \end{bmatrix} + \begin{bmatrix} \mathbf{0} \\ \mathbf{I}_{2\times 2} \end{bmatrix} \mathbf{U}_i \,, \quad (1)$$

where $\mathbf{x}_i = [\mathbf{P}_i, \dot{\mathbf{P}}_i]^\intercal$ is the state of the formation agent i and $\mathbf{U}_i = [U_{ix}, U_{iy}]^\intercal$, $i = 1, ..., N$ is its control input. Note that our centralized control design can access the state information of all agents. We model the robot-object links as free rotating joints. The goal is to drive the deformable object to a target configuration, that we set as a combination of shape, scale, position and orientation of the robotic formation. Our proposal to solve this problem is not to control explicitly the configuration of the object, but the configuration of the formation of robots that manipulate the object. This solution is especially useful for manipulating highly deformable objects, which adapt their structure closely to the shape of the formation, and for performing manipulation tasks that require many manipulators. We encode the target shape of the formation as

a set of positions $\mathbf{P}_{di} = [P_{dix}, P_{diy}]^\intercal$, $i = 1, ..., N$, that we stack in a matrix $\mathbf{P}_d = [\mathbf{P}_{d1}, \mathbf{P}_{d2}, ..., \mathbf{P}_{dN}] \in \mathbb{R}^{2 \times N}$. Without loss of generality and for simplicity, we define the target shape centered in the desired formation centroid $\mathbf{g}_d = \frac{1}{N}\mathbf{P}_d\,\mathbf{1}_N$. The target formation scale is s_d and the target formation orientation is θ_d. Then, we define the target configuration as

$$\mathbf{P}_T = s_d\mathbf{R}_d(\theta_d)(\mathbf{P}_d - \mathbf{g}_d\mathbf{1}_N^\intercal) + \mathbf{g}_d\mathbf{1}_N^\intercal \,, \quad (2)$$

where $\mathbf{R}_d(\theta_d) \in SO(2)$ is the 2D rotation matrix corresponding to an angle θ_d.

In addition, we consider that there are obstacles in the environment, which make agent-to-obstacle and object-to-obstacle collision avoidance mandatory requirements to reach the target configuration.

III. FORMATION CONTROL FOR AGENTS WITH DOUBLE-INTEGRATOR DYNAMICS

The control strategy we propose consists of a series of terms that are focused on controlling each one of the configuration parameters: shape, scale, position and orientation. In particular, the control of the first two variables, shape and scale, represents the object's deformation controller. Translation and rotation of the formation produce global movements that do not modify the relative positions of the agents, and therefore they do not deform the object.

A. Deformation control

In this section, we describe the shape and scale controllers.

Shape control. Firstly, in order to control the shape of the formation we define the following cost function [19]:

$$\gamma = \frac{1}{2}\|\mathbf{P}_b - \mathbf{H}\mathbf{P}_{db}\|_F^2 \,, \quad (3)$$

where $\|\cdot\|_F$ denotes the Frobenius norm,

$$\mathbf{P}_b = \mathbf{P} - \mathbf{g}\,\mathbf{1}_N^\intercal \,, \quad (4)$$

$$\mathbf{P}_{db} = \mathbf{P}_d - \mathbf{g}_d\mathbf{1}_N^\intercal \,, \quad (5)$$

$$\mathbf{H} = \begin{bmatrix} h_1 & -h_2 \\ h_2 & h_1 \end{bmatrix} \,. \quad (6)$$

$\mathbf{H}$ is a transformation matrix that optimally aligns $\mathbf{P}_b$ and $\mathbf{P}_{db}$, the matrices of all agents positions with zero centroid [6]. We compute the two terms h_1 and h_2 as follows:

$$h_1 = \frac{\text{tr}(\mathbf{P}_b\mathbf{P}_{db}^\intercal)}{\text{tr}(\mathbf{P}_{db}\mathbf{P}_{db}^\intercal)} \,, \quad h_2 = \frac{\text{tr}(\mathbf{P}_b(\mathbf{S}\mathbf{P}_{db})^\intercal)}{\text{tr}(\mathbf{P}_{db}\mathbf{P}_{db}^\intercal)} \,, \quad (7)$$

where $\mathbf{S} = [(0,1)^\intercal, (-1,0)^\intercal]$. The scale and orientation of the formation can be obtained from $\mathbf{H}$ as $s^2 = |\mathbf{H}|$ and $\theta = \text{atan2}(h_2, h_1) \in (-\pi, \pi]$ respectively, where the atan2 operator represents the four quadrant inverse tangent.

Cost function (3) provides a measure of the difference in shape between $\mathbf{P}_b$ and $\mathbf{P}_{db}$. Then, we propose the following shape controller that consists of a linear combination of the negative gradient of γ and the time derivative of the negative gradient of γ:

$$\mathbf{U}_H = -k_{1H}\nabla_{\mathbf{P}}\gamma - k_{2H}\frac{d(\nabla_{\mathbf{P}}\gamma)}{dt} =$$
$$= k_{1H}(\mathbf{H}\mathbf{P}_{db} - \mathbf{P}_b) + k_{2H}(\dot{\mathbf{H}}\mathbf{P}_{db} - \dot{\mathbf{P}}_b) \,, \quad (8)$$

where k_{1H} and k_{2H} are control gains. Controller (8), inspired by the one proposed by Fathian *et al.* ([8], eq. (22)), drives the formation of robots optimally to decrease γ and its time derivative, which implies a reduction of the difference in shape between the current $\mathbf{P}_b$ and the target $\mathbf{P}_{db}$. However, if the difference is large, since there is no control over the evolution of the shape from $\mathbf{P}_b$ to $\mathbf{P}_{db}$, $\mathbf{U}_H$ may switch the position of two neighboring robots. E.g., if the initial clockwise ordering of the positions in a three-agents formation is $\{1, 2, 3\}$, $\mathbf{U}_H$ may change it to $\{2, 1, 3\}$. Due to the fact that the formation is carrying an object, this kind of behavior could damage the object. We deal with this issue by defining a correction control term

$$\mathbf{U}_G = k_{1G}(\mathbf{P}_b \mathbf{P}_{db}^+ \mathbf{P}_{db} - \mathbf{P}_b) + k_{2G}(\dot{\mathbf{P}}_b \mathbf{P}_{db}^+ \mathbf{P}_{db} - \dot{\mathbf{P}}_b) \,, \quad (9)$$

where $\mathbf{P}_{db}^+$ is the right Moore-Penrose pseudoinverse of matrix $\mathbf{P}_{db}$ and k_{1G} and k_{2G} are control gains. This term is based on an optimal affine transformation that aligns $\mathbf{P}_{db}$ with $\mathbf{P}_b$, in a least-squares manner. For numerical reasons, $\mathbf{U}_G$ is compatible with any $\mathbf{P}_{db}$ different from a straight line, and it limits the movements of the agents to those that produce the deformation modes of stretch and shear. I.e. $\mathbf{U}_G$ steers the team towards the optimal affine deformation of $\mathbf{P}_{db}$ ($\mathbf{P}_b \mathbf{P}_{db}^+ \mathbf{P}_{db}$) and prevents those maneuvers that produce undesired folds and twists [19]. Thus, we combine the control terms $\mathbf{U}_H$ and $\mathbf{U}_G$ as follows:

$$\mathbf{U}_\gamma = \alpha_H \mathbf{U}_H + \alpha_G \mathbf{U}_G \,, \quad (10)$$

where α_H and α_G are weights that regulate the contribution of each term. If the difference between $\mathbf{P}_b$ and $\mathbf{P}_{db}$ is large, α_G should be greater than α_H. Otherwise, a greater α_H can increase the convergence rate. $\mathbf{U}_\gamma$ represents the shape controller of the formation. This controller drives the formation to the desired shape $\mathbf{P}_{db}$ by applying deformations that are close to the stretch and shear affine modes, as we will prove next.

In order to prove the stability of the system under $\mathbf{U}_\gamma$, we will show the condition for the system matrix to be Hurwitz and also that the input matrix is constant. The closed-loop equation of the system (1) under $\mathbf{U}_\gamma$ has, for the ith agent and with $\mathbf{x}_{bi} = [\mathbf{P}_{bi}, \dot{\mathbf{P}}_{bi}]^\mathsf{T}$, the form

$$\dot{\mathbf{x}}_{bi} = \mathbf{A}\mathbf{x}_{bi} + \mathbf{B} = \begin{bmatrix} 0 & 1 \\ a_{21} & a_{22} \end{bmatrix} \mathbf{x}_{bi} + \begin{bmatrix} 0 \\ b_2 \end{bmatrix} , \quad (11)$$

where

$$a_{21} = -\alpha_H k_{1H} + \alpha_G k_{1G}(\mathbf{P}_{dbi}^+ \mathbf{P}_{dbi} - 1) \,, \quad (12)$$
$$a_{22} = -\alpha_H k_{2H} + \alpha_G k_{2G}(\mathbf{P}_{dbi}^+ \mathbf{P}_{dbi} - 1) \,, \quad (13)$$
$$b_2 = \alpha_H(k_{1H}\mathbf{HP}_{dbi} + k_{2H}\dot{\mathbf{H}}\mathbf{P}_{dbi}) \,. \quad (14)$$

The roots of the system matrix $\mathbf{A}$ are computed as

$$\lambda = \frac{1}{2}(-\alpha_H k_{2H} + \alpha_G k_{2G}\mathbf{P}_{dbi}^+ \mathbf{P}_{dbi} - \alpha_G k_{2G}$$
$$\pm ((\alpha_H k_{2H} - \alpha_G k_{2G}\mathbf{P}_{dbi}^+ \mathbf{P}_{dbi} + \alpha_G k_{2G})^2$$
$$- 4(\alpha_H k_{1H} - \alpha_G k_{1G}\mathbf{P}_{dbi}^+ \mathbf{P}_{dbi} + \alpha_G k_{1G}))^{\frac{1}{2}}) \,. \quad (15)$$

For $\mathbf{A}$ to be Hurwitz, the real part of its roots must satisfy $\text{Re}(\lambda) < 0$. Regarding the input matrix $\mathbf{B}$, note that $\dot{\mathbf{H}} = \mathbf{0}$ under $\mathbf{U}_\gamma$, as we prove later. Then, $\mathbf{B}$ is a constant matrix. Therefore, if we set the control parameters so that $\mathbf{A}$ is Hurwitz, the system is asymptotically stable under the controller $\mathbf{U}_\gamma$. In Section V we report example values of the control parameters such that $\text{Re}(\lambda) < 0$.

We will show that s, θ and $\mathbf{g}$ are invariant under $\mathbf{U}_\gamma$. We start with s and θ, by obtaining

$$\ddot{h}_1 = \text{tr}(\mathbf{P}_{db}\mathbf{P}_{db}^\mathsf{T})^{-1}\text{tr}(\ddot{\mathbf{P}}_b\mathbf{P}_{db}^\mathsf{T}) = \text{tr}(\mathbf{P}_{db}\mathbf{P}_{db}^\mathsf{T})^{-1}\text{tr}(\mathbf{U}_\gamma\mathbf{P}_{db}^\mathsf{T})$$
$$= \text{tr}(\mathbf{P}_{db}\mathbf{P}_{db}^\mathsf{T})^{-1}\text{tr}(\alpha_H(k_{1H}(\mathbf{HP}_{db}\mathbf{P}_{db}^\mathsf{T} - \mathbf{P}_b\mathbf{P}_{db}^\mathsf{T})$$
$$+ k_{2H}(\dot{\mathbf{H}}\mathbf{P}_{db}\mathbf{P}_{db}^\mathsf{T} - \dot{\mathbf{P}}_b\mathbf{P}_{db}^\mathsf{T}))$$
$$+ \alpha_G(k_{1G}(\mathbf{P}_b\mathbf{P}_{db}^\mathsf{T}(\mathbf{P}_{db}\mathbf{P}_{db}^\mathsf{T})^{-1}\mathbf{P}_{db}\mathbf{P}_{db}^\mathsf{T} - \mathbf{P}_b\mathbf{P}_{db}^\mathsf{T})$$
$$+ k_{2G}(\dot{\mathbf{P}}_b\mathbf{P}_{db}^\mathsf{T}(\mathbf{P}_{db}\mathbf{P}_{db}^\mathsf{T})^{-1}\mathbf{P}_{db}\mathbf{P}_{db}^\mathsf{T} - \dot{\mathbf{P}}_b\mathbf{P}_{db}^\mathsf{T}))) \,. \quad (16)$$

Taking the derivative of $\text{tr}(\mathbf{P}_b\mathbf{P}_{db}^\mathsf{T}) = \text{tr}(\mathbf{HP}_{db}\mathbf{P}_{db}^\mathsf{T})$ [19], we obtain $\text{tr}(\dot{\mathbf{P}}_b\mathbf{P}_{db}^\mathsf{T}) = \text{tr}(\dot{\mathbf{H}}\mathbf{P}_{db}\mathbf{P}_{db}^\mathsf{T})$. We apply these relations in (16) to get $\ddot{h}_1 = 0$. By following the same procedure for $\ddot{h}_2$, we obtain $\ddot{h}_2 = 0$, which yields $\ddot{\mathbf{H}} = \mathbf{0}$. Given that the controller acts over accelerations and assuming that the system is at rest at initial time, we determine that $\dot{\mathbf{H}} = \mathbf{0}$ and $\mathbf{U}_\gamma$ does not modify s and θ.

Scale control. At this point, we are able to control the shape of the object carried by the formation of robots, but for controlling the deformation of the object we must control also the scale of the formation. We propose the following controller:

$$\mathbf{U}_s = -k_{1s}e_s(1/s)\mathbf{HP}_{db} - k_{2s}\dot{\mathbf{P}}_b \,, \quad (17)$$

where k_{1s} and k_{2s} are control gains and $e_s = s - s_d$ is the scale error. This controller produces a uniform scaling of the goal shape $\mathbf{HP}_{db}$ which is proportional to the scale error and the velocity of the agents. Then, we define the deformation controller $\mathbf{U}_D$ as the addition of the shape and scale controllers:

$$\mathbf{U}_D = \mathbf{U}_\gamma + \mathbf{U}_s \,. \quad (18)$$

B. Full controller with translation and rotation control

As we highlighted previously, translation and rotation of the formation produce global motions that do not affect the shape and scale of the team. We consider a scheme similar to $\mathbf{U}_s$ for the translation $\mathbf{U}_g$ and rotation $\mathbf{U}_\theta$ controllers:

$$\mathbf{U}_g = -k_{1g}\mathbf{e}_g\mathbf{1}_N^\mathsf{T} - k_{2g}\dot{\mathbf{P}} \,, \quad (19)$$
$$\mathbf{U}_\theta = -k_{1\theta}e_\theta\mathbf{SHP}_{db} - k_{2\theta}\dot{\mathbf{P}}_b \,, \quad (20)$$

where k_{1g}, k_{2g}, $k_{1\theta}$ and $k_{2\theta}$ are control gains, $\mathbf{e}_g = \mathbf{g} - \mathbf{g}_d$ is the formation centroid's position error and $e_\theta = \theta - \theta_d$ is the formation orientation error. $\mathbf{U}_g$ is essentially a standard proportional controller for double-integrator dynamics, and $\mathbf{U}_\theta$ is a control term that applies the desired orientation θ_d to the target shape. We prove next that $\mathbf{g}$ is invariant under

$\mathbf{U}_\gamma$. The acceleration of $\mathbf{g}$ is computed as

$$\ddot{\mathbf{g}} = \frac{1}{N}\ddot{\mathbf{P}}\,\mathbf{1}_N = \frac{1}{N}(\alpha_H(k_{1H}(\mathbf{HP}_{db} - \mathbf{P}_b) \\ + k_{2H}(\dot{\mathbf{H}}\mathbf{P}_{db} - \dot{\mathbf{P}}_b)) + \alpha_G(k_{1G}(\mathbf{P}_b\mathbf{P}_{db}^+\mathbf{P}_{db} - \mathbf{P}_b) \\ + k_{2G}(\dot{\mathbf{P}}_b\mathbf{P}_{db}^+\mathbf{P}_{db} - \dot{\mathbf{P}}_b)))\mathbf{1}_N \,. \quad (21)$$

By definition, we know that $\mathbf{P}_{db}\,\mathbf{1}_N = \mathbf{0}$, $\mathbf{P}_b\,\mathbf{1}_N = \mathbf{0}$ and $\dot{\mathbf{P}}_b\,\mathbf{1}_N = \mathbf{0}$. Thus, $\ddot{\mathbf{g}} = \mathbf{0}$, and $\mathbf{g}$ is invariant under $\mathbf{U}_\gamma$.

Then, we propose the full formation controller

$$\mathbf{U}_f = \mathbf{U}_D + \mathbf{U}_g + \mathbf{U}_\theta \,, \quad (22)$$

which represents a linear combination of the deformation, translation and rotation controllers. In the next section, we define a set of linear constraints based in CBFs that allow us to guarantee a safe state of the system at all times.

IV. SAFE CONTROL WITH CBFs

A. Collision avoidance

Due to the fact that the previous controller does not take into account explicitly collision avoidance, we need an additional strategy to complement the formation controller $\mathbf{U}_f$. Collisions may occur: between two agents (agent-to-agent), between an agent and an obstacle (agent-to-obstacle) and between the object and an obstacle (object-to-obstacle). In contrast to other multirobot systems, where the agents are not linked by a solid structure, collision avoidance is more challenging in our case: the robots are grasping the object, and their maneuvers must always respect the admissible deformation states of the object. Control barrier functions (CBFs) provide a robust, flexible and minimally invasive solution to this issue. We adapt and extend the centralized formulation proposed by Wang et al. [20], for collision avoidance in a team of robots that are assigned different position goals. Our system can be written in the affine form

$$\dot{\mathbf{x}}_{ij} = f(\mathbf{x}_{ij}) + g(\mathbf{x}_{ij})\mathbf{U}_{ij} \,, \quad (23)$$

where $\mathbf{x}_{ij} = [\mathbf{P}_{ij}, \dot{\mathbf{P}}_{ij}]^\intercal$, $\mathbf{P}_{ij} = \mathbf{P}_i - \mathbf{Q}_j$, $\mathbf{U}_{ij} = \mathbf{U}_i - \mathbf{W}_j$ and $f(\mathbf{x}_{ij})$ and $g(\mathbf{x}_{ij})$ are locally Lipschitz continuous functions, which describe how the agents are coupled with each other via the controller. Note that $\mathbf{Q}_j$ and $\mathbf{W}_j$ are the position and control input, respectively, of agent j, which can be a robot of the formation (and then $\mathbf{Q}_j = \mathbf{P}_j$, $\mathbf{W}_j = \mathbf{U}_j$) or an obstacle. In the latter case, we must set $\mathbf{W}_j = \mathbf{0}$ (obstacles cannot be controlled). Then, we propose the following condition for collision avoidance, which restricts the distance between i and j to a minimum value:

$$\|\mathbf{P}_{ij}\| + \int_{t_0}^{t_f} \dot{P}_{ij}^\perp(t)dt \geq D_{ij}^{min} \,, \quad (24)$$

where

$$\dot{P}_{ij}^\perp = \frac{\mathbf{P}_{ij}^\intercal}{\|\mathbf{P}_{ij}\|}\dot{\mathbf{P}}_{ij} \quad (25)$$

is the normal component of the relative velocity $\dot{\mathbf{P}}_{ij}$,

$$t_f = \frac{\dot{P}_{ij}^\perp(t_f) - \dot{P}_{ij}^\perp(t_0)}{\alpha_i + \alpha_j} + t_0 \quad (26)$$

for $\dot{P}_{ij}^\perp(t_f) = 0$ is the time instant after having applied the maximum braking accelerations α_i and α_j ($\|\ddot{\mathbf{P}}_i\|_\infty = \alpha_i$), and D_{ij}^{min} is the minimum allowed distance between i and j. If j is an obstacle, $\alpha_j = 0$. After manipulation of the previous equations, and taking $t_0 = 0$, we get the candidate CBF for i and j

$$h_{ij} = 2(\alpha_i + \alpha_j)(\|\mathbf{P}_{ij}\| - D_{ij}^{min}) - \dot{P}_{ij}^{\perp 2} \,, \quad (27)$$

which is defined in $\mathbb{R}$ for both the safe and the unsafe regions. By definition [21], we know that $h_{ij}(\mathbf{x}_{ij})$ is a CBF if there exists an extended class K_∞ function $\varepsilon(h_{ij}(\mathbf{x}_{ij}))$ such that

$$\sup_{\mathbf{U}_{ij}}[L_f h_{ij}(\mathbf{x}_{ij}) + L_g h_{ij}(\mathbf{x}_{ij})\mathbf{U}_{ij}] \geq -\varepsilon(h_{ij}(\mathbf{x}_{ij})) \,, \quad (28)$$

where L represents the Lie derivative. By using this definition and substituting our candidate CBF (27), we obtain a set of linear constraints with respect to $\mathbf{U}_{ij}$:

$$\mathbf{P}_{ij}^\intercal\dot{\mathbf{P}}_{ij}\frac{\mathbf{P}_{ij}^\intercal}{\|\mathbf{P}_{ij}\|}\mathbf{U}_{ij} \leq (\alpha_i + \alpha_j)\mathbf{P}_{ij}^\intercal\dot{\mathbf{P}}_{ij} + \frac{\|\mathbf{P}_{ij}\|}{2}\varepsilon(h_{ij}) \,. \quad (29)$$

These constraints guarantee that the system will maintain a minimal distance of D_{ij}^{min} between the center of agent i and the center of agent/obstacle j. This implies that agents and obstacles are circles with regard to collision avoidance. However, if $\|\mathbf{P}_{ab}\| \geq D_{ac}^{min} + D_{bc}^{min}$, where a and b are neighboring agents and c an obstacle, c could penetrate into the formation. This behavior is undesired in the present case, because it would result in an object-to-obstacle collision.

The strategy we propose to solve this issue consists in deploying a set of virtual agents $\mathbf{P}_{vk} = [P_{vkx}, P_{vky}]^\intercal$, $k = 1, ..., V$ over the contour edges of the formation polygon. These virtual agents add new distance constraints with respect to the obstacles, and their virtual inputs are computed as the linear combination

$$\mathbf{U}_{vk} = (1 - \nu)\,\mathbf{U}_i + \nu\,\mathbf{U}_j \,, \quad (30)$$

where $\nu = \|\mathbf{P}_{vk} - \mathbf{P}_i\|/\|\mathbf{P}_j - \mathbf{P}_i\|$ and $\mathbf{P}_{vk}$ is the position of the virtual agent in the edge $\overline{ij}$. This strategy preserves the desired safety distance D_{ij}^{min}. In addition, the computational cost of the system does not increase substantially, since no new control inputs are added (the virtual inputs are computed from the ones of the real agents).

B. Overstretching avoidance

Yet minimally invasive over $\mathbf{U}_f$, the collision avoidance system may separate two agents beyond the deformation limit of the carried object. We can write the condition to avoid overstretching the object as a restriction on the maximum distance between i and j:

$$\|\mathbf{P}_{ij}\| + \int_{t_0}^{t_f} \dot{P}_{ij}^\perp(t)dt \leq D_{ij}^{max} \,, \quad (31)$$

where

$$t_f = \frac{\dot{P}_{ij}^\perp(t_0)}{\alpha_i + \alpha_j} - t_0 \quad (32)$$

and D_{ij}^{max} is the maximum allowed separation between i and j. Note that this distance can be set differently for each

pair of agents, so that more fragile parts of the object are constrained to a higher extent than the rest. The following CBF candidate integrates the previous equations as

$$h'_{ij} = 2(\alpha_i + \alpha_j)(D_{ij}^{max} - \|\mathbf{P}_{ij}\|) - \dot{P}_{ij}^{\perp 2} . \quad (33)$$

By substituting (33) in (28) we get the new set of constraints

$$\frac{\mathbf{P}_{ij}^\mathsf{T}}{\|\mathbf{P}_{ij}\|}\dot{\mathbf{P}}_{ij}\mathbf{P}_{ij}^\mathsf{T}\mathbf{U}_{ij} \leq -(\alpha_i + \alpha_j)\mathbf{P}_{ij}^\mathsf{T}\dot{\mathbf{P}}_{ij} + \frac{\|\mathbf{P}_{ij}\|}{2}\varepsilon'(h'_{ij}) . \quad (34)$$

These constraints prevent stretching the object more than D_{ij}^{max} between every pair of agents i and j.

C. Quadratic-programming based controller

Finally, we introduce the previous constraints into a quadratic-programming (Q-P) based controller, which outputs the safe control inputs $\mathbf{U} = [\mathbf{U}_1^\mathsf{T}, \mathbf{U}_2^\mathsf{T}, ..., \mathbf{U}_N^\mathsf{T}]^\mathsf{T} \in \mathbb{R}^{2N}$:

$$\text{Given} \quad \mathbf{U}_f, \mathbf{P}, \dot{\mathbf{P}}, D_{ij}^{min}, D_{ij}^{max}, \alpha_i, \alpha_j$$

$$\underset{\mathbf{U}}{\text{minimize}} \quad \xi = \sum_{i=1}^{N} \|\mathbf{U}_i - \mathbf{U}_{fi}\|_2^2 \quad (35)$$

subject to:

$$\mathbf{A}_{ij}\mathbf{U} \leq b_{ij} , \forall i \neq j, \ i = 1, ..., N, \ j = 1, ..., N + M ,$$
$$\mathbf{A}_{kj}\mathbf{U} \leq b_{kj} , \ k = 1, ..., V, \ j = 1, ..., M ,$$
$$\mathbf{A}'_{ij}\mathbf{U} \leq b'_{ij} , \forall i \neq j, \ i = 1, ..., N, \ j = 1, ..., N ,$$
$$\|\mathbf{U}_i\|_\infty \leq \alpha_i, i = 1, ..., N$$

where M is the number of obstacles, $\mathbf{A}_{ij}$, $\mathbf{A}_{kj}$ and $\mathbf{A}'_{ij}$ are defined as

$$\mathbf{A}_{**} = [0, ..., \mathbf{P}_{**}^\mathsf{T}\dot{\mathbf{P}}_{**}\frac{\mathbf{P}_{**}^\mathsf{T}}{\|\mathbf{P}_{**}\|}, ..., -\mathbf{P}_{**}^\mathsf{T}\dot{\mathbf{P}}_{**}\frac{\mathbf{P}_{**}^\mathsf{T}}{\|\mathbf{P}_{**}\|}, ..., 0] , \quad (36)$$

being subscript $**$ the corresponding indexes and the first non-zero terms in the i_{th}/k_{th} position and the second in the j_{th} position,

$$b_{ij} = (\alpha_i + \alpha_j)\mathbf{P}_{ij}^\mathsf{T}\dot{\mathbf{P}}_{ij} + \frac{\|\mathbf{P}_{ij}\|}{2}\varepsilon(h_{ij}) , \quad (37)$$

$$b_{kj} = ((1 - \nu)\alpha_i + \nu\,\alpha_j)\mathbf{P}_{kj}^\mathsf{T}\dot{\mathbf{P}}_{kj} + \frac{\|\mathbf{P}_{kj}\|}{2}\varepsilon(h_{kj}) , \quad (38)$$

$$b'_{ij} = -(\alpha_i + \alpha_j)\mathbf{P}_{ij}^\mathsf{T}\dot{\mathbf{P}}_{ij} + \frac{\|\mathbf{P}_{ij}\|}{2}\varepsilon'(h'_{ij}) . \quad (39)$$

The Q-P based controller computes, for each agent, the closest control input $\mathbf{U}_i$ to the nominal $\mathbf{U}_{fi}$ that satisfies the collision and overstretching avoidance constraints.

V. SIMULATION RESULTS

A. Comparison between $\mathbf{U}_f$ and the Q-P based controller

We evaluate the performance and robustness of our proposal in two different simulation scenarios, created in Matlab®. The first scenario allows us to test the formation controller and the Q-P based controller in a standard transport task. We consider a team of $N = 4$ robots that transport a rectangular deformable sheet, in an environment with two static obstacles. This sheet is modeled in 3D with the As-Rigid-As-Possible (ARAP) technique [22], but we focus on the configuration of its 2D projection on the horizontal plane. The goal is to drive the object from an initial squared configuration to a rectangular target configuration, in a different place and with different orientation. Agent-to-agent, agent-to-obstacle and object-to-obstacle collisions must be avoided, as well as excessively stretching the object. The control parameters are configured so that they satisfy $\text{Re}(\lambda) < 0$: $k_{1H} = 4$, $k_{2H} = 2$, $k_{1G} = 4$, $k_{2G} = 2$, $\alpha_H = 1$, $\alpha_G = 10$, $k_{1s} = 3$, $k_{2s} = 1$, $k_{1g} = 0.2$, $k_{2g} = 1$, $k_{1\theta} = 3$, $k_{2\theta} = 1$, $\varepsilon = 3\,h_{ij}$, $\varepsilon' = h'_{ij}$, $s_d = 1$, $\theta_d = 0$ and the control time step is 0.01 [s]. Note that the method does not need fine tuning of the parameters to achieve a satisfactory performance. For uniformity purposes, $\alpha_i = 5$ [m/s²], $D_{ij}^{min} = 1 + d_r$ [m], where $d_r = 0.35$ [m] is the diameter of the robots (considered as circles), and $D_{ij}^{max} = 5$ [m] $\forall i \neq j$. We also include 16 virtual agents, evenly distributed in the formation contour edges. We compare two cases: the system with $\mathbf{U}_f$ *as is* and the system with $\mathbf{U}$ from the Q-P based controller, which includes $\mathbf{U}_f$ and the CBFs. Figure 2 shows the results in the two cases. The first image, at the left, shows that $\mathbf{U}_f$ steers the system successfully to the desired configuration of the formation. However, the obstacle is not evaded, and it penetrates into the formation. This undesirable event is corrected in the second case with the CBFs, from the second to the fourth image at the right, and the target configuration is still achieved. In both cases, we can see that the robots deform the object without compromising its structural integrity, thanks to $\mathbf{U}_G$ and the overstretching avoidance CBF.

B. Test with perturbations and dynamic obstacles

In the second scenario we test a challenging transport task, which includes three obstacles, two dynamic and one static, and perturbations acting over the controller. We assume that we can measure the position and velocity of the obstacles, and we set the perturbations as random noise applied to $\mathbf{U}$ for modeling sensing and actuation errors, in the range $[-0.05\,\alpha_i, 0.05\,\alpha_i]$. We consider a team of $N = 5$ robots, and the goal is to steer the deformable sheet from a square to a pentagonal shape, in a different place and with different orientation. The control parameters are configured as in the previous experiment, but $D_{ij}^{min} = 0.5 + d_r$ [m] for the agent-to-agent collision avoidance (for the agent-to-obstacle and object-to-obstacle collision avoidance, $D_{ij}^{min} = 1 + d_r$ [m]), we include 15 virtual agents and the control time step is slowed down to 0.03 [s]. Figure 3 shows eight different simulation instants of the system in the test scenario. We can see that the controller steers the formation to $\mathbf{P}_T$ without collisions. The admissible deformation states are preserved, and excessive stretching is also avoided. Notice that when the existing constraints force the team to deform, this deformation is affine (see Fig. 3, third from the left at the top). Figure 4 depicts the values of γ and the control errors. If the level of noise in the control input is high, it might be necessary to increase the safety distance in order to guarantee
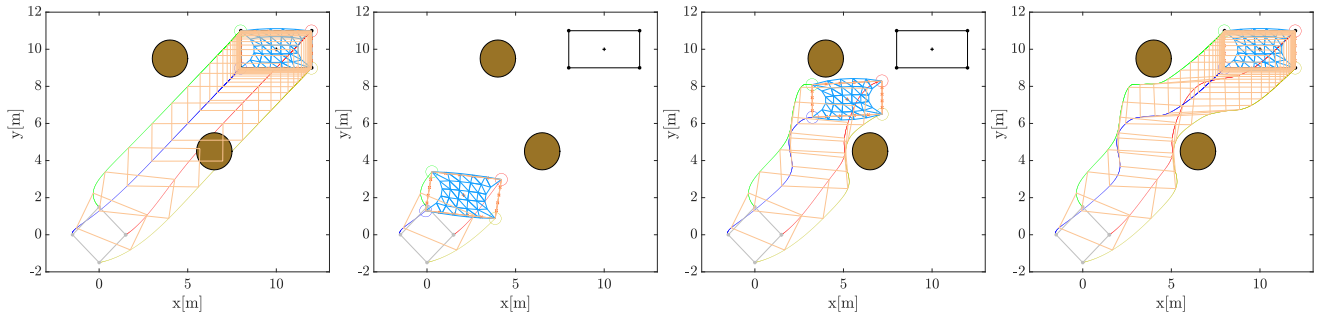
Fig. 2. The goal is to drive the formation of 4 robots (orange) and the object (blue mesh) from the initial configuration $\mathbf{P}$ at $(0,0)$ to the target configuration $\mathbf{P}_T$ (black) at $(10,10)$. In the first simulation (left image) $\mathbf{P}_T$ is reached at $t = 25$ [s] but the CFBs are not active, and the collision with the lower obstacle (brown circle) is not avoided. In the second simulation (2nd to 4th images, $t = 2, 8, 20$ [s]), $\mathbf{P}_T$ is reached without collisions. Sixteen virtual agents are represented as orange '$\times$'. We also depict the robots trajectories and the formation shape at even intervals.
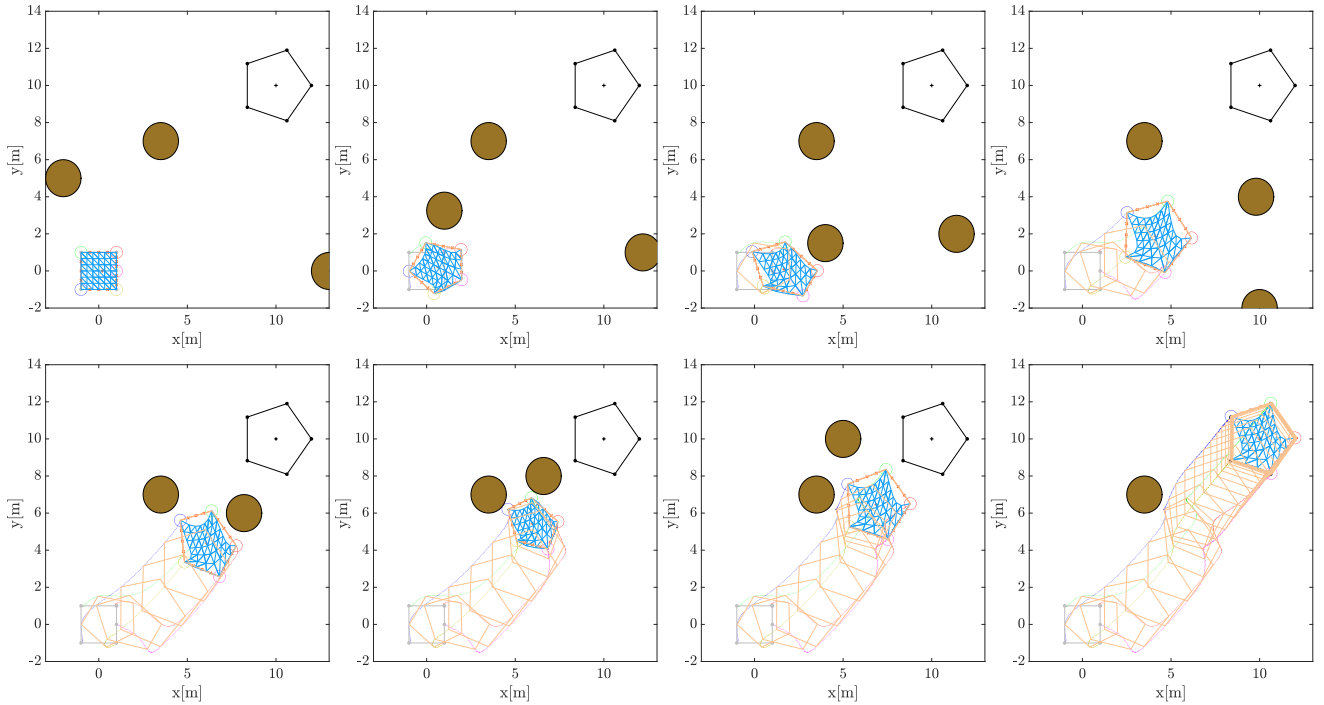
Fig. 3. The goal is to drive the formation of robots and the object from the initial configuration $\mathbf{P}$ at $(0,0)$ to the target configuration $\mathbf{P}_T$ at $(10,10)$ with challenging conditions: noise applied to $\mathbf{U}$ and dynamic obstacles. From left to right and from top to bottom, we show eight different simulation instants ($t = 0, 1, 2, 4, 6, 8, 10, 40$ [s]). We can see that the system avoids all kinds of collisions to reach $\mathbf{P}_T$ safely. Overstretching is also prevented, and deformation states of the object are restricted to the admissible modes.
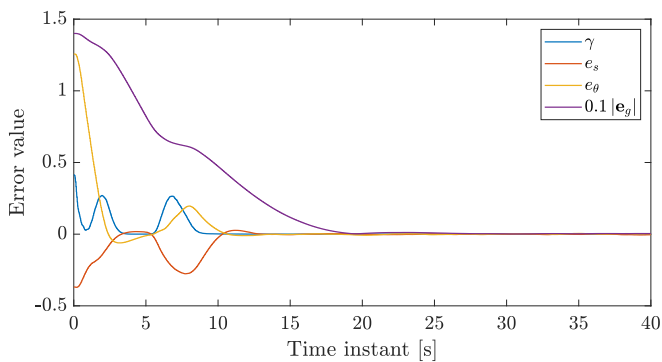
Fig. 4. Values of γ, e_s, e_θ and $0.1|\mathbf{e}_g|$ in the test with perturbations and dynamic obstacles.

collision avoidance at all times. In these tests, the execution of (35) takes around 3 [ms] to resolve, on average.

We include additional material in the attached video.

VI. CONCLUSION

We have presented a formation controller for agents with double-integrator dynamics that allows steering a team of robots to a desired configuration. Due to the fact that the robots carry a 2D deformable object, CBFs are defined to avoid agent-to-agent, agent-to-obstacle and object-to-obstacle collisions, as well as to prevent overstretching the object. Simulation results of the integrated Q-P based controller show good performance of the method in a challenging scenario with perturbations and dynamic obstacles.

REFERENCES

[1] J. Sanchez, J. A. Corrales, B. C. Bouzgarrou, and Y. Mezouar, "Robotic manipulation and sensing of deformable objects in domestic and industrial applications: a survey," *The International Journal of Robotics Research*, vol. 37, no. 7, pp. 688–716, 2018.

[2] H. Yin, A. Varava, and D. Kragic, "Modeling, learning, perception, and control methods for deformable object manipulation," *Science Robotics*, vol. 6, no. 54, p. eabd8803, 2021.

[3] Z. Feng, G. Hu, Y. Sun, and J. Soon, "An overview of collaborative robotic manipulation in multi-robot systems," *Annual Reviews in Control*, vol. 49, pp. 113–127, 2020.

[4] R. Herguedas, G. Lopez-Nicolas, R. Aragues, and C. Sagues, "Survey on multi-robot manipulation of deformable objects," in *IEEE International Conference on Emerging Technologies and Factory Automation (ETFA)*, 2019, pp. 977–984.

[5] K.-K. Oh, M.-C. Park, and H.-S. Ahn, "A survey of multi-agent formation control," *Automatica*, vol. 53, pp. 424–440, 2015.

[6] M. Aranda, J. A. Corrales, and Y. Mezouar, "Deformation-based shape control with a multirobot system," in *IEEE International Conference on Robotics and Automation (ICRA)*, 2019, pp. 2174–2180.

[7] D. V. Dimarogonas and K. J. Kyriakopoulos, "A connection between formation infeasibility and velocity alignment in kinematic multi-agent systems," *Automatica*, vol. 44, no. 10, pp. 2648–2654, 2008.

[8] K. Fathian, T. H. Summers, and N. R. Gans, "Robust distributed formation control of agents with higher-order dynamics," *IEEE Control Systems Letters*, vol. 2, no. 3, pp. 495–500, 2018.

[9] Z. Lin, L. Wang, Z. Chen, M. Fu, and Z. Han, "Necessary and sufficient graphical conditions for affine formation control," *IEEE Transactions on Automatic Control*, vol. 61, no. 10, pp. 2877–2891, 2016.

[10] S. Zhao, "Affine formation maneuver control of multiagent systems," *IEEE Transactions on Automatic Control*, vol. 63, no. 12, pp. 4140–4155, 2018.

[11] S. Zhao, D. V. Dimarogonas, Z. Sun, and D. Bauso, "A general approach to coordination control of mobile agents with motion constraints," *IEEE Transactions on Automatic Control*, vol. 63, no. 5, pp. 1509–1516, 2018.

[12] J. Felix-Rendon, J. C. Bello-Robles, and R. Q. Fuentes-Aguilar, "Control of differential-drive mobile robots for soft object deformation," *ISA Transactions*, vol. 117, pp. 221–233, 2021.

[13] J. Alonso-Mora, R. Knepper, R. Siegwart, and D. Rus, "Local motion planning for collaborative multi-robot manipulation of deformable objects," in *IEEE International Conference on Robotics and Automation (ICRA)*, 2015, pp. 5495–5502.

[14] D. McConachie, A. Dobson, M. Ruan, and D. Berenson, "Manipulating deformable objects by interleaving prediction, planning, and control," *The International Journal of Robotics Research*, vol. 39, no. 8, pp. 957–982, 2020.

[15] G. Lopez-Nicolas, R. Herguedas, M. Aranda, and Y. Mezouar, "Simultaneous shape control and transport with multiple robots," in *IEEE International Conference on Robotic Computing (IRC)*, 2020, pp. 218–225.

[16] A. Hegde and D. Ghose, "Multi-UAV collaborative transportation of payloads with obstacle avoidance," *IEEE Control Systems Letters*, vol. 6, pp. 926–931, 2022.

[17] A. Clark, "Control barrier functions for stochastic systems," *Automatica*, vol. 130, p. 109688, 2021.

[18] K. A. Hamed, V. R. Kamidi, W.-L. Ma, A. Leonessa, and A. D. Ames, "Hierarchical and safe motion control for cooperative locomotion of robotic guide dogs and humans: A hybrid systems approach," *IEEE Robotics and Automation Letters*, vol. 5, no. 1, pp. 56–63, 2020.

[19] M. Aranda, J. Sanchez, J. A. Corrales Ramon, and Y. Mezouar, "Robotic motion coordination based on a geometric deformation measure," *IEEE Systems Journal*, 2021, doi: 10.1109/JSYST.2021.3107779.

[20] L. Wang, A. D. Ames, and M. Egerstedt, "Safety barrier certificates for collisions-free multirobot systems," *IEEE Transactions on Robotics*, vol. 33, no. 3, pp. 661–674, 2017.

[21] A. D. Ames, S. Coogan, M. Egerstedt, G. Notomista, K. Sreenath, and P. Tabuada, "Control barrier functions: Theory and applications," in *European Control Conference (ECC)*, 2019, pp. 3420–3431.

[22] O. Sorkine and M. Alexa, "As-Rigid-as-Possible surface modeling," in *Proceedings of the Fifth Eurographics Symposium on Geometry Processing*. Eurographics Association, 2007, pp. 109–116.